Looking for evidence of mixing in the solar wind from 0.31 to 0.98 AU

Joseph E. Borovsky[1,2]

Received 11 January 2012; revised 26 April 2012; accepted 8 May 2012; published 27 June 2012.

[1] To determine the efficacy of turbulence in the solar wind, the amount of mixing of the solar wind plasma is quantified. If magnetohydrodynamic turbulence in the solar wind acts as does Navier-Stokes turbulence, the chunk mixture of scalar quantities in the solar wind plasma should evolve with time. In particular, (1) the sizes of plasma chunks should decrease with distance from the Sun owing to the stretching and folding action of turbulence and (2) the occurrence distributions of passive-scalar values in the plasma should narrow with distance from the Sun owing to homogenization. The evolution of the chunk mix is studied through the use of interface-crossing statistics. Using Helios 1 and Helios 2 slow-solar wind measurements from 0.31 to 0.98 AU, temporal jumps in the proton number density, proton specific entropy, and proton beta are used to locate plasma interfaces in the solar wind and the plasma chunk sizes are determined from the distances between the plasma interfaces. No evidence for the evolution of the chunk-size distribution is seen, indicating an absence of mixing in the solar wind. The distribution of plasma density broadens by 11% with distance, the distribution of proton flux stays constant, while the distribution of proton specific entropy narrows by 14%; collectively the three distributions do not show clear evidence for evolution toward homogeneity, hence they do not show clear evidence for mixing. Implications of the lack of evidence for mixing in the solar wind are discussed.

Citation: Borovsky, J. E. (2012), Looking for evidence of mixing in the solar wind from 0.31 to 0.98 AU, *J. Geophys. Res.*, *117*, A06107, doi:10.1029/2012JA017525.

1. Introduction

[2] Mixing is a universal property of turbulence [*Liepmann*, 1979; *Ottino*, 1990; *Dimotakis*, 2000; *Shraiman and Siggia*, 2000; *Abarzhi and Sreenivasan*, 2010]. Measurements of mixing can shed light on the physics of turbulence [*Gibson*, 1991; *Holzer and Siggia*, 1994; *Sreenivasan and Antonia*, 1997; *Warhaft*, 2000; *Shraiman and Siggia*, 2000] and turbulent mixing has many practical applications that call for quantification of mixing rates [cf. *Paul et al.*, 2003]. The solar wind is believed to be turbulent and measurements of mixing could shed light on the nature of the turbulence and on the effectiveness of the turbulence.

[3] Mixing is usually studied by examining the evolution of a passive scalar in the fluid. (A "passive scalar" is a scalar quantity that is convected by the fluid without perturbing the fluid behavior.) Studies of Navier-Stokes fluids have led to the concept that there are three temporal stages to turbulent mixing [cf. *Eckart*, 1948; *Huq and Britter*, 1995; *Villermaux and Innocenti*, 1999; *Shraiman and Siggia*, 2000; *Kresta and Brodkey*, 2003; *Dimotakis*, 2000, 2005]: (1) entrainment, (2) stretching and folding, and (3) diffusion. (These three stages are also denoted as macromixing, mesomixing, and micromixing [cf. *Paul et al.*, 2003].) In stages (1) and (2) the turbulence forms a "chunk mix" of the passive scalar [*Cheng et al.*, 2003; *Cheng*, 2009] with the thicknesses of the chunks lying within the inertial subrange of spatial scales, and the thicknesses decreasing with time owing to stretching and the chunks becoming more plentiful owing to folding [*Corrsin*, 1959; *Ottino*, 1990; *Yee et al.*, 1995a; *Yeung*, 2002; *Brethouwer et al.*, 2003]. The chunk boundaries are delineated by passive-scalar interfaces, and the distances between adjacent passive-scalar interfaces decreases with time during these stages [*Stapountzis et al.*, 1986; *Ottino et al.*, 1988; *Shraiman and Siggia*, 2000]. Visualizing the analogy of a bucket of paint initially half white paint and half red paint, upon stirring the "chunks" seen in the bucket would be striations of color, stretching and folding and rapidly becoming thinner and thinner. In stage (3) the chunk thickness and interface separations approach a diffusion scale wherein diffusion destroys the structures [*Garrett*, 1983; *Dahm et al.*, 1991; *Buch and Dahm*, 1996, 1998] and homogenizes the fluid. Visualizing again the bucket of red and white paint, in stage 2 the red and white striations disappear and all appears pink.

[4] The mixing time τ_{mix} of the turbulence is typically defined as a timescale for the fluid to approach homogeneity

[1]Department of Atmospheric, Oceanic, and Space Sciences, University of Michigan, Ann Arbor, Michigan, USA.
[2]Space Science Institute, Boulder, Colorado, USA.

Corresponding author: J. E. Borovsky, PO Box 661, Los Alamos, NM 87544, USA. (jborovsky@spacescience.org)

0148-0227/12/2012JA017525

[cf. *Kramers et al.*, 1953; *Voth et al.*, 2003; *Hartmann et al.*, 2006], i.e., the time for fluctuations in the passive-scalar concentration to form, multiply, and decay. In Navier-Stokes turbulence the mixing time τ_{mix} is observed to be on the order of the eddy-turnover time τ_{eddy} for large eddies [*Prochazka and Landau*, 1961; *McKelvey et al.*, 1975; *Durban*, 1982; *Eswaran and Pope*, 1988; *Shraiman and Siggia*, 2000; *Kresta and Brodkey*, 2003] with some dependence of τ_{mix} on the initial scale sizes of the passive scalar field [cf. *Villermaux et al.*, 1998; *Ristorcelli*, 2006] and with only slight dependence of τ_{mix} on the Reynolds number of the turbulence [cf. *Fox and Gex*, 1956, Figure 6; *Norwood and Metzner*, 1960, Figures 7 and 8; *Prochazka and Landau*, 1961, Figure 4; *Livescu et al.*, 2000, Figure 25]. Sometimes the mixing time τ_{mix} is taken to be the eddy-diffusion timescale [cf. *Seale*, 1979; *Rehme*, 1992], which is approximately an eddy-turnover timescale τ_{eddy}. For timescales less than to on the order of the mixing time, one expects to see the scalar chunk mix in the fluid developing increasing complexity with smaller and smaller scale sizes as time increases. Also, during these timescales one expects the distribution of passive-scalar values to narrow toward homogeneity.

[5] The slow solar wind shows substantial density-temperature structure [*Bame et al.*, 1977; *Schwenn*, 1990; *Ofman*, 2004], unlike the coronal-hole-origin fast wind that can be quasi-homogeneous for days. In the solar wind scalar quantities such as temperature, density, ion composition, and specific entropy should be advected by turbulence and should show evidence of mixing as the fluid ages. In the slow solar wind the turbulence is thought to be well developed [e.g., *Luttrell and Richter*, 1988; *Marsch and Tu*, 1990a, 1990b], owing to an absence of a strong outward imbalance of Alfvénic fluctuations [e.g., *Tu et al.*, 1990; *Klein et al.*, 1993; *Bruno*, 1997; *Horbury and Schmidt*, 1999]. In the fast wind it has been argued that the turbulence is young, with the fluctuations dominated by outward traveling Alfvén waves that have not had sufficient time to join the turbulence cascade [*Tu et al.*, 1990; *Horbury and Schmidt*, 1999]. The turbulence age of the slow solar wind at 1 AU has been estimated to be a few eddy turnover times [*Roberts et al.*, 1992; *Goldstein et al.*, 1995; *Matthaeus et al.*, 1998]: for example, taking $v_{rms} = 14$ km/s for the large eddy velocity [cf. *Borovsky and Funsten*, 2003, Table 1] and $L_{corr} = 1.4 \times 10^6$ km as the large-eddy scale size [cf. *Wicks et al.*, 2010] yields $\tau_{eddy} \sim L_{corr}/v_{rms} = 28$ h at 1 AU, which compares with the ~100-h age of the wind at 1 AU. If MHD turbulence in a collisionless plasma operates in a fashion similar to Navier-Stokes turbulence, one should expect to see a mixing evolution of the solar wind plasma with increasing distance from the Sun out to 1 AU. If no mixing is found, there could be important implications for the solar wind.

[6] Using Helios plasma measurements from 0.31 AU to 0.98 AU the chunk-size statistics in the inertial subrange of the slow solar wind will be examined as a function of distance from the Sun. (See section 5 for a discussion of plasma chunks in the solar wind.) Evidence for mixing as the plasma ages will be sought.

[7] This manuscript is organized as follows. In section 2 the data sets and data-analysis methods are discussed. In section 3 the statistical analysis of the time-intervals between plasma interfaces is performed and interpreted. In section 4 occurrence distributions for scalar quantities in the solar wind are examined and interpreted. Section 5 contains discussion about the shapes of plasma chunks in the solar wind and about the potential effects of the acceleration, compression, and rarefaction of the solar wind. The study is summarized in section 6 and implications of the results are discussed.

2. Data Analysis Methods

[8] To look for evidence of mixing, merged plasma and magnetic field data from Helios 1 and Helios 2 [*Rosenbauer et al.*, 1977; *Denskat and Neubauer*, 1982] from 0.31 to 0.98 AU is analyzed. Subintervals of slow wind ($v_{sw} <$ 425 km/s) with nearly continuous 40-s time-resolution data coverage are collected. To be included in the analysis, a subinterval must be at least 0.15-day (3.6-h) in length. The 0.15-day limit is chosen for two reasons: (1) the "inertial subrange" for magnetic field fluctuations in the Helios slow-wind data set spans frequencies higher than $\sim 10^{-4}$ Hz [cf. *Roberts*, 2010, Figures 3 and 5] corresponding to timescales shorter than ~3 h and (2) probably owing to the diurnal telemetry schedule for the Helios mission, there are a lot of data intervals that are ~0.15-days long. For Helios 1, measurements from January 1975 to April 1977 are utilized, and for Helios 2, measurements from January 1976 to March 1977 are utilized; after these dates the data sets are subject to density-temperature bimodal oscillations. Subintervals of slow wind in which the solar wind speed briefly exceeds 425 km/s were kept, however if the wind speed went above 425 km/s and stayed above, the interval was terminated at the point where the speed crossed 425 km/s. 231 data subintervals are collected comprising 1754 h of measurements: the shortest interval is 3.61 h, the longest is 45.6 h, the median length is 5.8 h, and the mean length is 7.6 h. In Figure 1 (top) the occurrence distribution of the distance r from the Sun is shown for all of the measurements inside the 231 data subintervals: 44% of the measurements lie in the range 0.80–0.98 AU, 29% lie in the range 0.41–0.79 AU, and 27% lie in the range 0.31–0.40 AU. The occurrence distribution of the solar wind velocity v_{sw} for all of the Helios 1 and 2 measurements within the 231 data subintervals is plotted in Figure 1 (bottom): the mean value is 349 km/s and the median value is 352 km/s.

[9] In Figure 2 the time-of-flight age of the solar wind r/v_{sw} is binned for the Helios 1 and 2 measurements in three ranges of distance from the Sun: 0.31–0.40 AU (red curve with solid points), 0.41–0.79 AU (green curve with hollow points), and 0.80–0.98 AU (blue curve with square points). The mean values of the age in the three ranges are 41 h, 73 h, and 104 h as noted on the plot along with the standard deviations of the ages.

[10] In the 231 data subintervals, plasma interfaces are located by two methods: manual and automated. To manually locate the plasma interfaces temporal plots of the plasma parameters n_p (proton number density), S_p (proton specific entropy $T_p/n_p^{2/3}$) [*Bernstein et al.*, 1958; *Kulsrud*, 1983; *Schindler and Birn*, 1978], and β_p (proton beta $8\pi n k_B T_p/B^2$) are examined and temporal discontinuities one or two points wide in the plotted plasma parameters are marked manually. This method has the advantage that the eye is a good noise

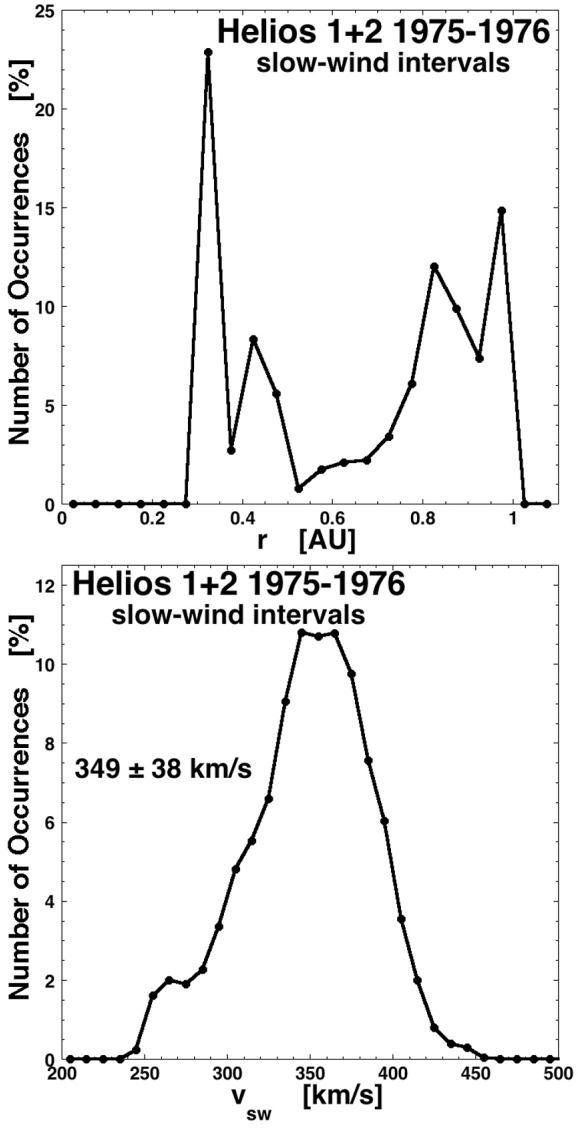

Figure 1. The occurrence distributions of distance from the (top) Sun and (bottom) solar wind speed v_{sw} for all of the 40-s time-resolution measurements in the 231 data subintervals of slow solar wind analyzed.

filter and edges can be discerned through noisy data. The approximate criteria for edge selection are $\Delta\log_{10}(n_p) > \log_{10}(1.2)$, $\Delta\log_{10}(S_p) > \log_{10}(1.4)$, and β_p changing substantially (i.e., from low-beta to high-beta or vice versa). If an edge is found in any of the three parameters, a plasma interface is marked. Two drawbacks to the manual method are that it is subjective and that it is time consuming. Only 96 of the 231 subintervals were analyzed manually, all from Helios 1.

[11] The automated method of locating plasma interfaces uses a 4-point algorithm to calculate the temporal change in the logarithm of a plasma parameter "p":

$$\Delta\log_{10}(p) = [\log_{10}(p_{i+1}) + \log_{10}(p_i)]/2.0 - [\log_{10}(p_{i-1}) + \log_{10}(p_{i-2})]/2.0 \quad (1)$$

Four points are used instead of two-point differences to reduce sensitivity of the triggering to noise in the plasma data. Interfaces are marked whenever $\Delta\log_{10}(n_p) > \log_{10}(1.2)$, whenever $\Delta\log_{10}(S_p) > \log_{10}(1.5)$, or whenever $\Delta\log_{10}(\beta_p) > \log_{10}(2.5)$. These trigger values were adequately high to prevent noise from dominating the triggering. When the 4-point algorithm of expression (1) produces triggers at adjacent data points, the location of the interface is taken to be the location with the largest value of $\Delta\log_{10}(p)$. All 231 subintervals were analyzed with the automated method.

[12] Once the plasma interfaces are located, the time intervals Δt between subsequent interfaces is determined and the collection of Δt values is analyzed. The Δt values are interpreted to be the sizes of chunks in the chunk mix.

[13] In analyzing the Δt values, only values 2 min $\leq \Delta t \leq$ 110 min is utilized. Values of $\Delta t <$ 2 min (with a 4-point algorithm on 40-s data) are interpreted to be multiple triggers or noise. With the data subintervals having lengths as short as 0.15 day = 3.6 h = 216 min, measurements of Δt values (requiring the locating of two plasma interfaces) that are much longer than half a subinterval length (108 min) long will be interfered with by the finite subinterval duration. Hence, the 110-min upper limit.

3. Plasma-Interface Statistics and Interpretation

[14] The statistics of passive-scalar interfaces in a turbulent fluid can be used to study the physics of the turbulence and the physics of mixing [e.g., *Prasad and Sreenivasan*, 1989, 1990; *Miller and Dimotakis*, 1991; *Catrakis*, 2000; *Catrakis et al.*, 2002; *Catrakis and Aguirre*, 2004; *Dasi et al.*, 2007]. One method to detect and quantify mixing is to examine the one-dimensional distribution of time intervals or distances between interface crossings along straight-line paths through the turbulent fluid [cf. *Sreenivasan et al.*, 1983, Figure 13; *Prasad and Sreenivasan*, 1990, Figure 15; *Kerstein*, 1991, Figure 2; *Yee et al.*, 1995b, Figures 11 and 12; *Catrakis and Bond*, 2000, Figure 6]. The interface crossings along the path of a spacecraft through the advecting solar wind plasma suffice as such a line. Owing to stretching

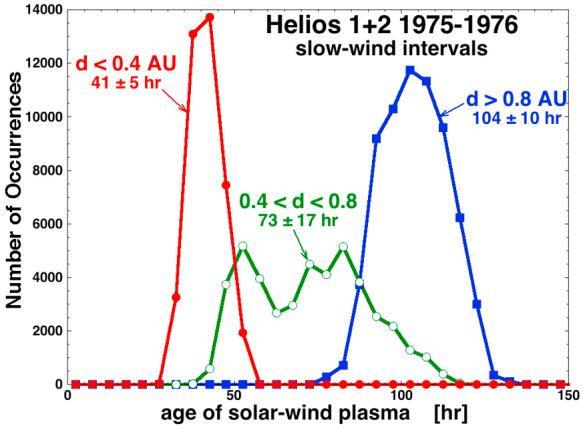

Figure 2. For all of the 40-s time-resolution measurements in the 231 data subintervals, the distribution of the age of the solar wind r/v_{sw} is plotted for three ranges of distances from the Sun (labeled).

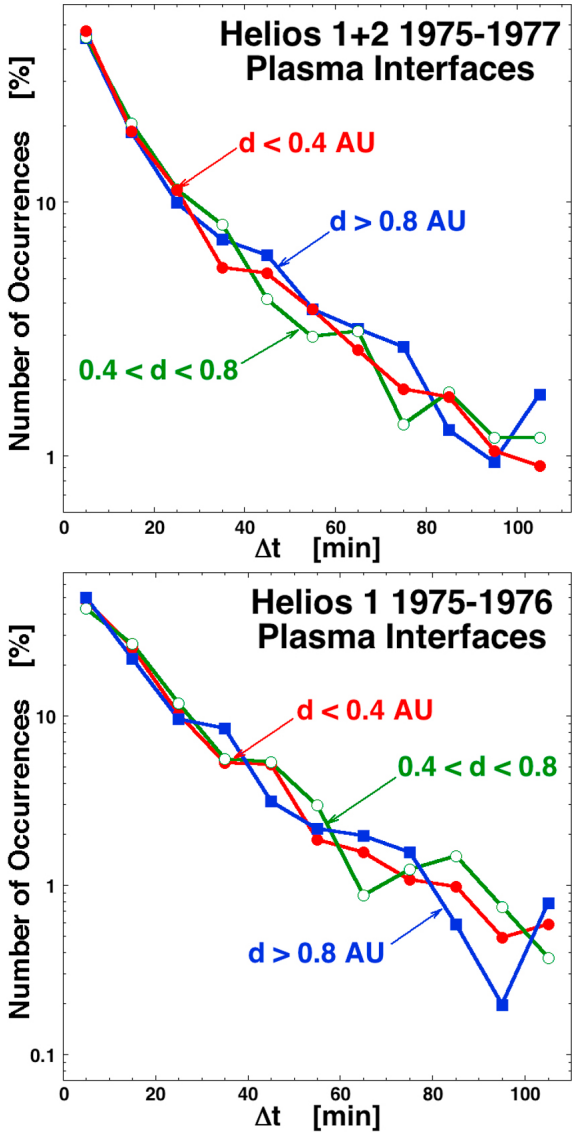

Figure 3. (top) The occurrence distributions of the time intervals Δt between subsequent plasma interfaces for interfaces that are found by the automated algorithm. (bottom) The occurrence distributions of the time intervals between subsequent plasma interfaces for interfaces that are found manually. The blue curves with square points are for spacecraft measurements between 0.8 and 0.98 AU, the green curves with hollow points are for spacecraft measurements between 0.41 and 0.79 AU, and the red curves with filled points are for spacecraft measurements between 0.31 and 0.40 AU.

and folding, the distances between passive-scalar interfaces in a turbulent fluid become smaller as time increases [*Stapountzis et al.*, 1986; *Ottino et al.*, 1988; *Shraiman and Siggia*, 2000] (see especially *Corrsin* [1959, Figure 7]).

[15] To look for evidence of mixing in the solar wind plasma, the distances between plasma interfaces are examined as a function of distance from the Sun, which is equivalent to as a function of the age of the solar wind plasma. These distances between interfaces represent the distribution of "chunk sizes" in the solar wind plasma. Under the action of turbulent mixing, we expect the chunk sizes in the solar wind plasma to decrease with distance from the Sun. The fundamental quantity to measure is the time interval Δt between subsequent plasma interface crossings by the spacecraft as the solar wind plasma is advected radially outward.

[16] In Figure 3 (top) the occurrence distributions of time intervals Δt for the plasma interfaces located by the automated algorithm (expression (1)) are plotted. Time intervals from 2 min to 110 min are binned for three different ranges of distance from the Sun: 0.31–0.40 AU (red curve with solid points), 0.41–0.79 AU (green curve with hollow points), and 0.80–0.98 AU (blue curve with square points). These chunk sizes are in the inertial subrange of the MHD turbulence of the solar wind, where stretching and folding is expected to act. As can be seen by comparing the three distributions in Figure 3 (top), the distribution of chunk sizes does not show any evident evolution from ~0.3 AU to ~1 AU, which is about a factor of 3 in the age of the solar wind plasma (see Figure 2). Hence, no evidence for mixing is found. The three distributions in Figure 3 (top) are consistent with a non-evolution of the plasma chunks from 0.3 AU to 1 AU.

[17] In Figure 3 (bottom) the occurrence distributions of time intervals Δt between subsequent plasma interfaces are plotted for the Helios plasma interfaces found manually. Again, the blue curve with square points is for 0.8–0.98 AU, the green curve with hollow points is for 0.41–0.79 AU, and the red curve with solid points is for 0.31–0.40 AU. And again, no evidence for mixing is seen in the chunk-size distributions as the solar wind advects out from 0.31 to 0.98 AU.

[18] As another view of the plasma chunk sizes, the time intervals Δt between subsequent interfaces are each converted to a chunk radial thickness Δx via $\Delta x = v_{sw}\Delta t$ using the measured value of the solar wind speed v_{sw} at the end of each time interval Δt. In the two panels of Figure 4 the occurrence distributions of these chunk radial thicknesses are plotted for the three distance ranges 0.31–0.40 AU (red curves with solid points), 0.41–0.79 AU (green curves with hollow points), and 0.80–0.98 AU (blue curves with square points) for interfaces located with the automated algorithm (top panel) and for interfaces located manually (bottom panel). In each panel of Figure 4, a comparison between the three curves again finds no evidence for the evolution of the chunk-size distribution with distance from the Sun. Hence, no evidence for mixing of the solar wind plasma is found.

4. Evolution of the Density and Specific-Entropy Probability Distribution Functions and Interpretation

[19] In the later stages of mixing (after an eddy-turnover time in Navier-Stokes) the evolution of a passive-scalar probability distribution function should reflect the evolution of the fluid toward homogeneity. In general this will take the form of a narrowing of the occurrence distribution function with time [*Eswaran and Pope*, 1988; *Yee et al.*, 1995b; *Livescu and Ristorcelli*, 2008], reflecting a decrease of the standard deviation of the fluctuations with increasing time [*Corrsin*, 1957; *McKelvey et al.*, 1975; *Newman et al.*, 1977;

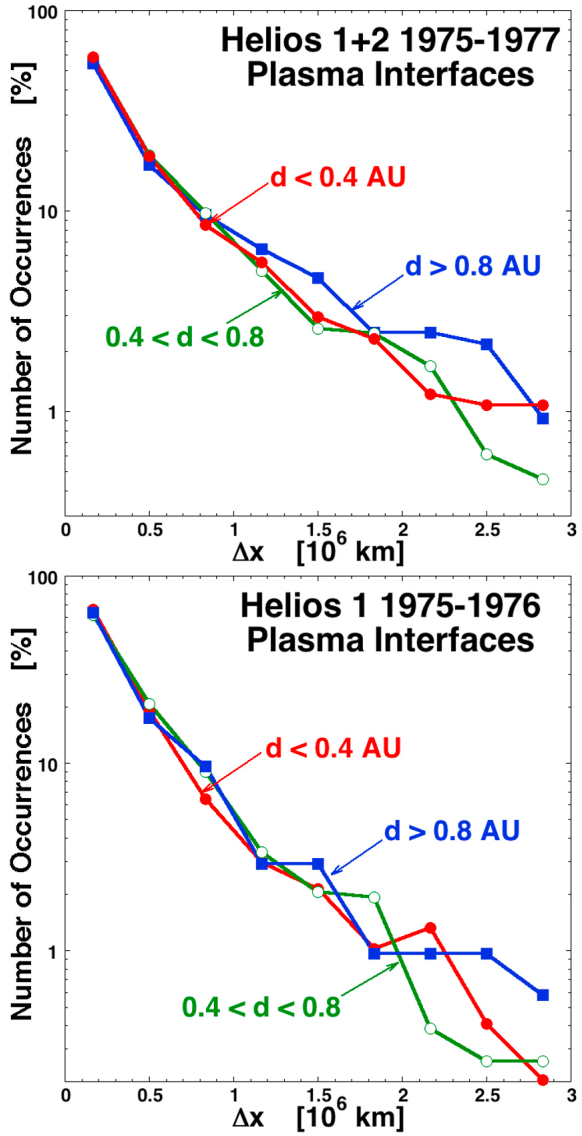

Figure 4. (top) The occurrence distributions of the radial distances between subsequent plasma interfaces for interfaces that are found by the automated algorithm. (bottom) The occurrence distributions of the radial distances between subsequent plasma interfaces for interfaces that are found manually. The blue curves with square points are for spacecraft measurements between 0.8 and 0.98 AU, the green curves with hollow points are for measurements between 0.41 and 0.79 AU, and the red curves with filled points are for measurements between 0.31 and 0.40 AU.

Sreenivasan et al., 1980; *Durban*, 1982; *Eswaran and Pope*, 1988; *Yee et al.*, 1995a; *Ristorcelli*, 2006; *Lee et al.*, 2010]. Owing to the action of mixing, the evolution of the occurrence distributions of passive scalars in the solar wind should reflect a homogenization of the plasma.

[20] To look for evidence of mixing in the solar wind plasma the occurrence distribution of the distance-normalized proton density r^2n_p, the proton flux $r^2v_{sw}n_p$, and the occurrence distribution of the proton specific entropy $S_p = T_p/n^{2/3}$ are examined as a functions of distance from the Sun from 0.31 AU to 0.98 AU. The quantity r^2n_p is chosen since it is conserved in the expanding solar wind in the absence of acceleration or compression or rarefaction events. The proton flux is chosen because it is conserved even in the presence of solar wind acceleration (section 5) [cf. *Schwenn et al.*, 1981]. The specific entropy is chosen because it is not altered by compression-rarefaction events [*Goertz and Baumjohann*, 1991; *Borovsky and Cayton*, 2011] such as compressions in corotating interaction regions, rarefactions on the trailing edges of high-speed streams, or compressions and rarefactions owing to the actions of turbulence. Nor is the specific entropy altered by the expansion of the solar wind with distance. The specific entropy has been used previously to identify different regions of the solar wind [*Burlaga et al.*, 1990; *Crooker et al.*, 1996; *Burton et al.*, 1999; *Neugebauer et al.*, 2004; *Pagel et al.*, 2004; *Borovsky*, 2008; *Borovsky and Denton*, 2010] and to examine evolution issues in the solar wind [e.g., *Eyni and Steinitz*, 1978; *Freeman and Lopez*, 1985; *Marsch et al.*, 1989; *Whang et al.*, 1989; *Osherovich et al.*, 1997; *Gosling*, 1999; *Borovsky and Denton*, 2011]. The amplitudes, spectral indices, and outward-inward imbalance of the MHD fluctuations in the solar wind are strongly correlated with the value of the proton specific entropy [*Borovsky*, 2012].

[21] In Figure 5 (top) the occurrence distributions of the logarithm of r^2n_p in the 231 data subintervals are plotted for the three ranges of distance from the Sun: 0.31–0.40 AU in red (solid points), 0.41–0.79 AU in green (hollow points), and 0.80–0.98 AU in blue (square points). If turbulent mixing is acting to homogenize the solar wind plasma, then the occurrence distribution of $\log_{10}(r^2n_p)$ should narrow with distance from the Sun. As noted on the plot, the standard deviations of $\log_{10}(r^2n_p)$ are 0.18 in the distance range closest to the Sun, 0.20 in the middle range, and 0.20 in the distance range farthest from the Sun. Hence there is no evidence of a narrowing of the occurrence distribution with time: in fact an 11% broadening is seen. Hence there is no evidence for mixing occurring in the solar wind. The broadening could by caused by compressions and rarefactions of the solar wind increasing with distance.

[22] In Figure 5 (middle) the occurrence distributions of the logarithm of the proton flux $r^2v_{sw}n_p$ in the 231 data subintervals are plotted for the three ranges of distance from the Sun: 0.31–0.40 AU in red (solid points), 0.41–0.79 AU in green (hollow points), and 0.80–0.98 AU in blue (square points). The flux passing a point varies with time in the slow wind mostly because the density fluctuates (i.e., because the plasma is lumpy). If turbulent mixing is acting to homogenize the solar wind plasma, then the occurrence distribution of $\log_{10}(r^2n_p)$ should narrow with distance from the Sun. As noted on the plot, the standard deviations of $\log_{10}(r^2n_p)$ are 0.19 in the distance range closest to the Sun, 0.18 in the middle range, and 0.20 in the distance range farthest from the Sun. Hence there is no evidence of a narrowing of the occurrence distribution with time; hence there is no evidence for mixing occurring in the solar wind.

[23] In Figure 5 (bottom) the occurrence distributions of the logarithm of S_p in the 231 data subintervals are plotted for the three ranges of distance from the Sun: 0.31–0.40 AU

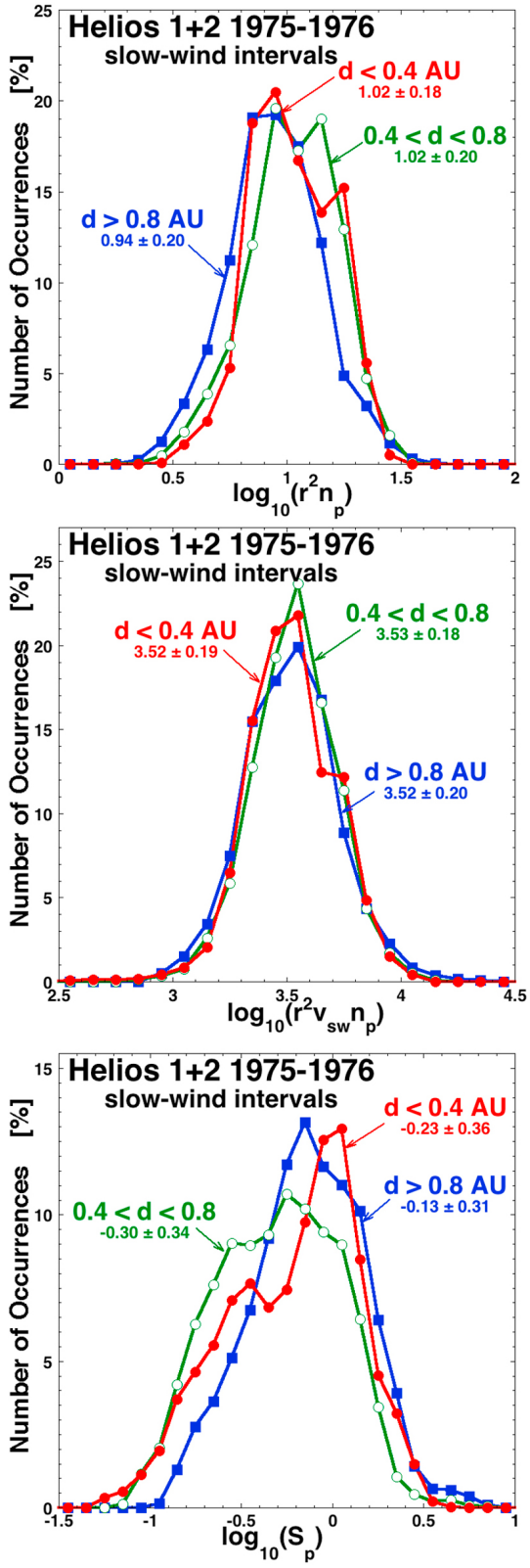

Figure 5. The occurrence distributions of the (top) distance-normalized proton density, (middle) the distance-normalized proton flux, and (bottom) the proton specific entropy are shown for various distance ranges from the Sun (colors as labeled). The mean values ± standard deviations of the logarithms are noted in the plots.

in red (solid points), 0.41–0.79 AU in green (hollow points), and 0.80–0.98 AU in blue (square points). If turbulent mixing is acting to homogenize the solar wind plasma, then the occurrence distribution of $\log_{10}(S_p)$ should narrow with distance from the Sun. As noted on the plot, the standard deviations of $\log_{10}(S_p)$ are 0.36 in the distance range closest to the Sun, 0.34 in the middle range, and 0.31 in the distance range farthest from the Sun. This is a 14% narrowing of the width of the occurrence distribution in the 0.39–0.98 AU range. The statistical significance of this 14% narrowing is weak, in light of the 11% widening of the $\log_{10}(r^2n_p)$ distribution in the top panel. Owing to the smallness of the narrowing and the contradiction by the $\log_{10}(r^2n_p)$ measurements, this narrowing will not be taken as clear evidence for homogenization of the slow wind with distance from the Sun, i.e., not taken as clear evidence for the occurrence of mixing.

[24] Note also in Figure 5 (bottom) that only weak evidence for the non-adiabatic heating of the slow-solar wind protons is seen in the three distributions of S_p: the near-adiabatic behavior of the slow solar wind in the Helios data set has been noted before [cf. *Eyni and Steinitz*, 1978; *Freeman and Lopez*, 1985; *Freeman*, 1988]. Non-adiabatic heating would produce an increase in the mean value of S_p with distance from the Sun: the logarithmically averaged values of S_p are $10^{-0.23} = 0.59$ eVcm^2 in the 0.31–0.40 AU range, $10^{-0.30} = 0.50$ eVcm^2 in the 0.41–0.79 AU, and $10^{-0.13} = 0.74$ eVcm^2 in the 0.8–0.98 AU range. This represents a 25% increase in the proton temperature over adiabatic cooling as the solar wind moves from 0.31 to 0.40 AU to 0.80–0.98 AU, however the measurements in the 0.41–0.79 AU range contradict this non-adiabatic heating trend.

5. Discussion

[25] It is safe to assume that the plasma structures (chunks) of the solar wind are filamentary [*Eselevich and Eselevich*, 2006; *Ogilvie et al.*, 2007]. Filamentary density structures are imaged near the Sun extending out to a fraction of an AU [*Hewish*, 1958; *Woo and Habbal*, 1997]. Magnetic field structure in the solar wind is known to be filamentary [*Bruno et al.*, 2001; *Borovsky*, 2010b] and aligned with the direction of the mean magnetic field [*Crooker et al.*, 1982; *Ridley*, 2000; *Bargatze et al.*, 2005], but there have been few tests of the orientation of plasma structures in the solar wind [cf. *Richardson and Paularena*, 1998, 2001]. Note, (1) that the plasma interfaces share the same strong current sheets as do the magnetic field structures (e.g., Figure 6 discussed in section 6) and (2) that the OMNI high-resolution solar wind data is the result of successfully propagating measurements of plasma density from upstream of the Earth to the Earth using the orientations of magnetic field structure [*Weimer and King*, 2008] (cf. http://omniweb.gsfc.nasa.gov/html/sc_merge_data1.html for details); these two observations both imply that the plasma is structured in filaments as is the magnetic field. The length of the plasma filaments in the solar wind is an unknown [cf. *Viall et al.*, 2010]. Investigation of the filamentary structure of the solar wind plasma (density, specific entropy, etc.) is left for a future study.

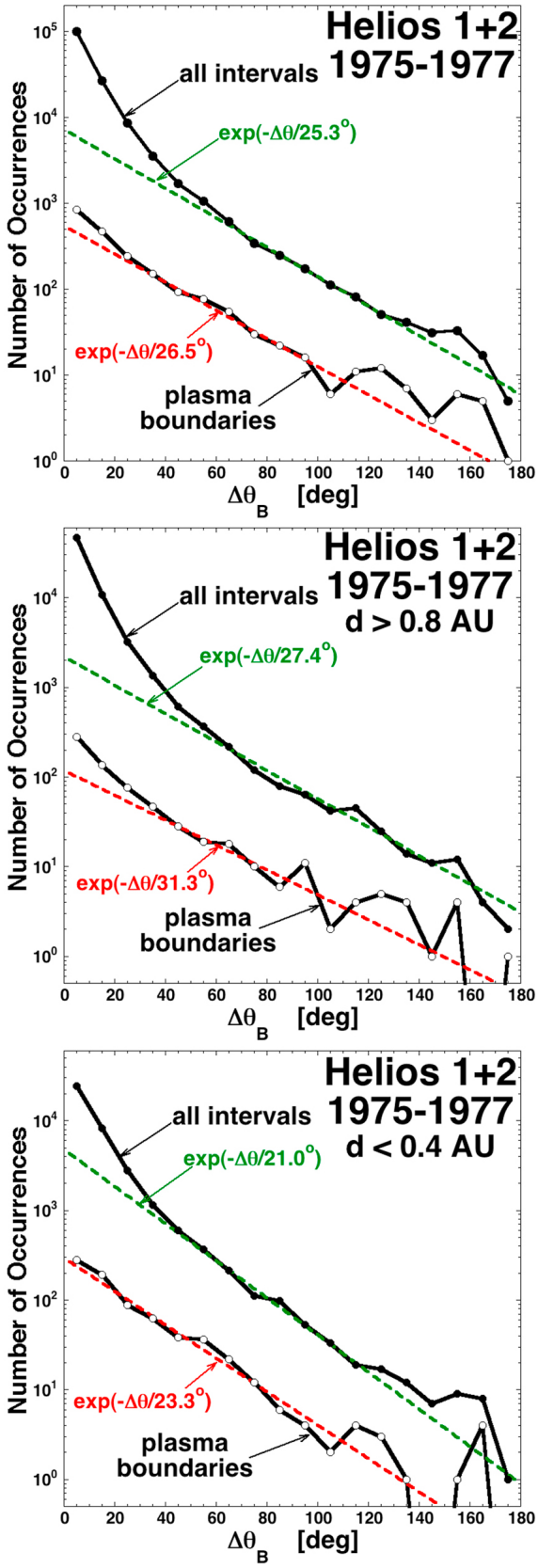

Figure 6. In each panel the top curve is the occurrence distribution of the 80-s magnetic field angular change $\Delta\theta_B$ for all measurements in the Helios 1 and 2 data subintervals and the bottom curve is the occurrence distribution of $\Delta\theta_B$ for measurements at plasma interfaces. (top) All distance from the Sun, (middle) 0.80–0.98 AU, and (bottom) 0.31–0.40 AU.

[26] Two processes in addition to turbulent mixing could act to evolve the plasma chunk-size distribution in the solar wind: acceleration of the wind and compression-rarefaction of the plasma. These two processes are discussed in this paragraph and the next. Most of the acceleration of the slow wind occurs within 60 R_s (=0.28 AU) of the Sun [cf. *Wang et al.*, 2000, Figure 7; *Breen et al.*, 2000, Figures 5–8; *Breen et al.*, 2002, Figure 2]. However, the Helios 1 and 2 measurements indicate that the slow component of the solar wind may further increase in speed by up to 25% from near 0.3 AU to near 1.0 AU [cf. *Schwenn et al.*, 1981, Figure 1; *Arya and Freeman*, 1991, Tables 1 and 3]. For non-evolving plasma structures, this increase in the solar wind speed with increasing distance from the Sun will produce an increase of the chunk sizes with increasing distance from the Sun, assuming that frequency (the number of events per unit time) is conserved. This acceleration will not change the Δt occurrence distribution (cf. Figure 3), but it will cause the Δx occurrence distribution to evolve with distance so that the plasma block sizes are up to 25% larger near 1 AU than they are near 0.3 AU. As pointed out by a reviewer, this may be the cause of the >0.8 AU curve being higher than the other two curves in Figure 4.

[27] Compressions and rarefactions of the solar wind plasma with distance will also produce changes in the distribution of plasma chunk sizes: compression with distance would tend to produce a chunk distribution that becomes smaller with distance and rarefaction with distance would tend to produce a chunk distribution that becomes larger with distance. This effect is probably weak in the Helios slow-wind data set used here. The chief source of compression of slow wind is at the leading edge of a corotating interaction region (CIR) where fast wind pushes against slow wind causing deflection and compression. As a gauge of CIR compression, examine the magnetic field strength at 1 AU plotted in *Borovsky and Denton* [2010, Figure 4] (or *Borovsky* [2010b, Figure 16]): appreciable compression of slow solar wind occurs for about 12 h prior to the passage of the stream interface. During that 12 h the solar wind velocity climbs from its unperturbed-slow-wind low value to about 450 km/s [see also *Borovsky and Denton*, 2010]. By the v_{sw} < 425 km/s selection criteria to choose slow wind, some of the weaker compressed wind during this 12-h interval could be chosen for the present mixing study but the stronger-compression wind would not be. Slow wind typically lasts for about 3 days prior to a CIR, so most of the slow wind is not in this compressed category. Hence, only a small fraction of slow wind will be compressed and that fraction not compressed strongly. Another source of large-scale solar wind compression is pushing of wind by fast CMEs: these should be rare in the 1975–1977 solar-minimum years studied here [*Ataç*, 1987; *Joshi and Joshi*, 2004], and,

as is the case for CIR compression, the compressed slow wind is pushed up in speed so that any strongly compressed portion would have $v_{sw} > 425$ km/s and would not be selected for the present study. On the issue of rarefaction, the chief rarefaction of the solar wind is on the trailing edge of high-speed streams. Examining the simulation in *Pizzo* [1978, Figure 11] one can see that (a) the rarefaction (in the density) on the trailing edge is mild and (b) the rarefaction is in the fast wind, which is likely not to be selected for the present study by the $v_{sw} < 425$ km/s criterion. Hence, compression and rarefaction of the solar wind plasma with distance probably does not have a strong impact on the evolution of the plasma chunk-size distribution.

6. Summary and Implications

[28] Five measurements were made to look for evidence of mixing in the solar wind: (1) the Δt chunk sizes of plasma versus distance from Sun, (2) the Δx chunk sizes of plasma versus distance from Sun, (3) the occurrence distribution of the distance-normalized proton density r^2n_p versus distance from the Sun, (4) the occurrence distribution of the proton flux $r^2v_{sw}n_p$ versus distance from the Sun, and (5) the occurrence distribution of the proton specific entropy S_p versus distance from the Sun. In these five measurements, the first four showed no evidence for mixing and the fifth showed only very weak evidence for mixing. The weak evidence came from the 14% reduction in the spread of the distribution of $\log_{10}(S_p)$ values going from 0.39 AU to 0.98 AU; this 14% narrowing of $\log_{10}(S_p)$ values was contradicted by an 11% increase in the spread of $\log_{10}(r^2n_p)$ values. Collectively, those two measurements yield no clear evidence for a homogenization of the solar wind plasma with age, i.e., no clear evidence for mixing.

[29] The question arises as to why there is not strong evidence for mixing in the solar wind. Three possibilities are discussed.

[30] The first possibility is that there is no turbulence in the solar wind; i.e., that the observed field and flow fluctuations of the solar wind are not produced by an active turbulence wherein the fluctuations interact nonlinearly with each other and evolve. Discerning turbulence from other structures in the solar wind has been an issue for decades [cf. *Siscoe et al.*, 1968; *Sari and Ness*, 1969; *Bavassano and Bruno*, 1991; *Tu and Marsch*, 1991, 1994, 1995; *Bruno and Carbone*, 2005; *Bruno et al.*, 2007; *Borovsky*, 2008; *Borovsky and Denton*, 2011; *Li et al.*, 2011; *Owens et al.*, 2011], and it has been argued that some types of solar wind fluctuations are fossils carried outward from the Sun [e.g., *Mariani et al.*, 1983; *Thieme et al.*, 1988, 1989, 1990; *Feldman et al.*, 1993; *Woo and Habbal*, 1998; *Reisenfeld et al.*, 1999; *Yamauchi et al.*, 2002, 2003; *Borovsky*, 2008]. The possibility has been raised that the majority of the Fourier power in the solar wind is owed to non-evolving fossil structure [cf. *Borovsky*, 2010a].

[31] A second possibility is that there is turbulence in the solar wind but with transport and mixing reduced by the restoring force (memory) of the solar wind mean magnetic field. Unlike the case of periodic-MHD simulations of turbulence, the effective line tying of the mean magnetic field into a distant plasma may prevent flux tubes from fully interchanging under the action of turbulence, preventing mixing from progressing even though flows may be stochastic.

[32] A third possibility is that there is turbulence in the solar wind but density, specific entropy, etc. do not act as passive scalars in the solar wind owing to strong magnetic shear at the plasma interfaces. This strong magnetic shear is demonstrated in Figure 6. The angular change $\Delta\theta_B$ in the magnetic field vector every 80 s is determined for all of the measurements in the 231 slow-wind data subintervals for Helios 1 and 2. In Figure 6 (top) the occurrence distribution of all of the $\Delta\theta_B$ values is plotted (top curve). As can be seen, the distribution has two components [cf. *Borovsky*, 2008, 2010b]: an exponential population of large-$\Delta\theta_B$ values (see the exponential fit in the plot) and a second population of small-$\Delta\theta_B$ values. The population of large-$\Delta\theta_B$ values represents locations in the solar wind plasma where there is strong magnetic shear. The occurrence distribution for measured $\Delta\theta_B$ values at the locations of the plasma interfaces in the Helios 1 and 2 slow wind is plotted as the lower curve in Figure 6 (top). As can be seen by comparing the two curves in the top panel, the plasma interfaces are synonymous with the population of strong magnetic shears. The plasma interfaces in the solar wind are characterized by strong magnetic shear: the mean value of $\Delta\theta_B$ across the interfaces is 23°. Strong magnetic shear is known to stabilize a plasma boundary to interchange and to transport [*Miura and Pritchett*, 1982; *Burrell*, 1997; *Matsumoto and Hoshino*, 2006]. It may be that the magnetic-shear on the plasma interfaces in the solar wind prevents any turbulent fluctuations in the plasma from producing mixing across the interface. Owing to the magnetic shears, the chunks of plasma in the solar wind could be robust and long-lived, perhaps non-evolving. In the middle and bottom plots of Figure 6 the populations of $\Delta\theta_B$ values are explored separately in the 0.80–0.98 AU range and in the 0.31–0.40 AU range. For both cases the plasma interfaces (bottom curves) are co-located with strong magnetic shears. Note from the fits to the distributions in the middle and bottom plots of Figure 6 that the magnetic-shear angles $\Delta\theta_B$ statistically increase with distance from the Sun: this increase can be explained by a transverse-to-radial expansion of the plasma chunks with distance from the Sun [*Borovsky*, 2010b].

[33] There are other indications in the literature that the action of turbulence in solar wind is weak. For one example, discrete-frequency periodic density oscillations are regularly seen at 1 AU in slow and fast solar wind [*Kepko and Spence*, 2003; *Villante et al.*, 2007; *Viall et al.*, 2009a] with periods of 3.5–25 min. Evidence is that they are of solar-surface origin [*Viall et al.*, 2009b], hence at 1 AU they are about 100 h old. Even though these periodic structures are in the inertial subrange of scale sizes, they are not destroyed (mixed away) by action of turbulence. For another example of the inaction of turbulence in the solar wind, eddy viscosity (momentum mixing) fails to broaden the long-lived velocity shears at CIR stream interfaces [*Borovsky*, 2006], which at 1 AU (100 h old) remain narrow [*Gosling et al.*, 1978].

[34] **Acknowledgments.** The author thanks Larry Kepko, John Podesta, Aaron Roberts, John Steinberg, Ruth Skoug, and Nicki Viall for helpful conversations. This work was supported by the NASA Heliospheric

SR&T Program, the NASA Heliospheric Guest-Investigator Program, and by the NSF SHINE Program.

[35] Philippa Browning thanks Nicholeen Viall and another reviewer for their assistance in evaluating this paper.

References

Abarzhi, S. I., and K. R. Sreenivasan (2010), Turbulent mixing and beyond, *Phil. Trans. R. Soc. A*, *368*, 1539, doi:10.1098/rsta.2010.0021.

Arya, S., and J. W. Freeman (1991), Estimates of solar wind velocity gradients between 0.3 and 1 AU based on velocity probability distributions from Helios 1 at perihelion and aphelion, *J. Geophys. Res.*, *96*, 14,183, doi:10.1029/91JA01135.

Ataç, T. (1987), Time variation of the flare index during the 21st solar cycle, *Astrophys. Space Sci.*, *135*, 201, doi:10.1007/BF00644477.

Bame, S. J., J. R. Asbridge, W. C. Feldman, and J. T. Gosling (1977), Evidence for a structure-free state at high solar wind speeds, *J. Geophys. Res.*, *82*, 1487, doi:10.1029/JA082i010p01487.

Bargatze, L. F., R. L. McPherron, J. Minamora, and D. Weimer (2005), A new interpretation of Weimer et al.'s solar wind propagation delay technique, *J. Geophys. Res.*, *110*, A07105, doi:10.1029/2004JA010902.

Bavassano, B., and R. Bruno (1991), Solar wind fluctuations at large scale: A comparison between low and high solar activity conditions, *J. Geophys. Res.*, *96*, 1737, doi:10.1029/90JA01959.

Bernstein, I. B., E. A. Friemen, M. D. Kruskal, and R. M. Kulsrud (1958), An energy principle for hydromagnetic stability problems, *Proc. R. Soc. London, Ser. A*, *244*, 17, doi:10.1098/rspa.1958.0023.

Borovsky, J. E. (2006), The eddy viscosity and flow properties of the solar wind: CIRs, CME sheaths, and solar-wind/magnetosphere coupling, *Phys. Plasmas*, *13*, 056505, doi:10.1063/1.2200308.

Borovsky, J. E. (2008), The flux tube texture of the solar wind: Strands of the magnetic carpet at 1 AU, *J. Geophys. Res.*, *113*, A08110, doi:10.1029/2007JA012684.

Borovsky, J. E. (2010a), Contribution of strong discontinuities to the power spectrum of the solar wind, *Phys. Rev. Lett.*, *105*, 111102, doi:10.1103/PhysRevLett.105.111102.

Borovsky, J. E. (2010b), On the variations of the solar wind magnetic field about the Parker spiral direction, *J. Geophys. Res.*, *115*, A09101, doi:10.1029/2009JA015040.

Borovsky, J. E. (2012), The velocity and magnetic-field fluctuations of the solar wind at 1 AU: Statistical analysis of Fourier spectra and correlations with plasma properties, *J. Geophys. Res.*, *117*, A05104, doi:10.1029/2011JA017499.

Borovsky, J. E., and T. E. Cayton (2011), Entropy mapping of the outer electron radiation belt between the magnetotail and geosynchronous orbit, *J. Geophys. Res.*, *116*, A06216, doi:10.1029/2011JA016470.

Borovsky, J. E., and M. H. Denton (2010), Solar-wind turbulence and shear: A superposed-epoch analysis of corotating interaction regions at 1 AU, *J. Geophys. Res.*, *115*, A10101, doi:10.1029/2009JA014966.

Borovsky, J. E., and M. H. Denton (2011), No evidence for heating of the solar wind at strong current sheets, *Phys. Rev. Lett.*, *739*, L61.

Borovsky, J. E., and H. O. Funsten (2003), Role of solar wind turbulence in the coupling of the solar wind to the Earth's magnetosphere, *J. Geophys. Res.*, *108*(A6), 1246, doi:10.1029/2002JA009601.

Breen, A. R., S. J. Tappin, C. A. Jordan, P. Thomasson, P. J. Moran, R. A. Fallows, A. Canals, and P. J. S. Williams (2000), Simultaneous interplanetary scintillation and optical measurements of the acceleration of the slow solar wind, *Ann. Geophys.*, *18*, 995, doi:10.1007/s00585-000-0995-9.

Breen, A. R., P. Thomasson, C. A. Jordan, S. J. Tappin, R. A. Fallows, A. Canals, and P. J. Moran (2002), Slow and fast solar wind acceleration near solar maximum, *Adv. Space Res.*, *30*, 433, doi:10.1016/S0273-1177(02)00339-3.

Brethouwer, G., J. C. R. Hunt, and F. T. M. Noeuwstadt (2003), Microstructure and Lagrangian statistics of the scalar field with a mean gradient in isotropic turbulence, *J. Fluid Mech.*, *474*, 193.

Bruno, R. (1997), Observations of MHD turbulence in the solar wind, *Nuovo Cimento Soc. Ital. Fis. C*, *20*, 881.

Bruno, R., and V. Carbone (2005), The solar wind as a turbulence laboratory, *Living Rev. Sol. Phys*, *2*, lrsp-2005-4.

Bruno, R., V. Carbone, P. Veltri, E. Pietropaolo, and B. Bavassano (2001), Identifying intermittency events in the solar wind, *Planet. Space Sci.*, *49*, 1201, doi:10.1016/S0032-0633(01)00061-7.

Bruno, R., R. D. D'Amicis, B. Bavassano, V. Carbone, and L. Sorriso-Valvo (2007), Magnetically dominated structures as an important component of the solar wind turbulence, *Ann. Geophys.*, *25*, 1913, doi:10.5194/angeo-25-1913-2007.

Buch, K. A., and W. J. A. Dahm (1996), Experimental study of the fine-scale structure of conserved scalar mixing in turbulent shear flows. Part 1. Sc >> 1, *J. Fluid Mech.*, *317*, 21, doi:10.1017/S0022112096000651.

Buch, K. A., and W. J. A. Dahm (1998), Experimental study of the fine-scale structure of conserved scalar mixing in turbulent shear flows. Part 2. Sc ≈ 1, *J. Fluid Mech.*, *364*, 1, doi:10.1017/S0022112098008726.

Burlaga, L. F., W. H. Mish, and Y. C. Whang (1990), Coalescence of recurrent streams of different sizes and amplitudes, *J. Geophys. Res.*, *95*, 4247, doi:10.1029/JA095iA04p04247.

Burrell, K. H. (1997), Effects of $E \times B$ velocity shear and magnetic shear on turbulence and transport in magnetic confinement devices, *Phys. Plasmas*, *4*, 1499, doi:10.1063/1.872367.

Burton, M. E., M. Neugebauer, N. U. Crooker, R. von Steiger, and E. J. Smith (1999), Identification of trailing edge solar wind stream interfaces: A comparison of Ulysses plasma and compositional measurements, *J. Geophys. Res.*, *104*, 9925.

Catrakis, H. J. (2000), Distribution of scales in turbulence, *Phys. Rev. E*, *62*, 564, doi:10.1103/PhysRevE.62.564.

Catrakis, H. J., and R. C. Aguirre (2004), Interfacial-fluid dynamics and the mixing efficiency of turbulent flows, *Phys. Fluids*, *16*, 4746, doi:10.1063/1.1811671.

Catrakis, H. J., and C. L. Bond (2000), Scale distributions of fluid interfaces in turbulence, *Phys. Fluids*, *12*, 2295, doi:10.1063/1.1286595.

Catrakis, H. J., R. C. Aguirre, J. Ruiz-Plancarte, and R. D. Thayne (2002), Shape complexity of whole-field three-dimensional space-time fluid interfaces in turbulence, *Phys. Fluids*, *14*, 3891, doi:10.1063/1.1505033.

Cheng, B. (2009), Review of turbulent mixing models, *Acta Math. Sci.*, *29*, 1703, doi:10.1016/S0252-9602(10)60012-4.

Cheng, B., J. Glimm, H. Jin, and D. Sharp (2003), Theoretical methods for the determination of mixing, *Lasers Part. Beams*, *21*, 429.

Corrsin, S. (1957), Simple theory of an idealized turbulent mixer, *AIChE J.*, *3*, 329, doi:10.1002/aic.690030309.

Corrsin, S. (1959), Outline of some topics in homogeneous turbulent flow, *J. Geophys. Res.*, *64*, 2134, doi:10.1029/JZ064i012p02134.

Crooker, N. U., G. L. Siscoe, C. T. Russell, and E. J. Smith (1982), Factors controlling degree of correlation between ISEE 1 and ISEE 3 interplanetary magnetic field measurements, *J. Geophys. Res.*, *87*, 2224, doi:10.1029/JA087iA04p02224.

Crooker, N. U., M. E. Burton, G. L. Siscoe, S. W. Kahler, J. T. Gosling, and E. J. Smith (1996), Solar wind streamer belt structure, *J. Geophys. Res.*, *101*, 24,331, doi:10.1029/96JA02412.

Dahm, W. J. A., K. B. Southerland, and K. A. Buch (1991), Direct, high resolution, four-dimensional measurements of the fine scale structure of Sc ≫ 1 molecular mixing in turbulent flows, *Phys. Fluids A*, *3*, 1115, doi:10.1063/1.858093.

Dasi, L. P., F. Schuerg, and D. R. Webster (2007), The geometric properties of high-Schmidt-number passive scalar iso-surfaces in turbulent boundary layers, *J. Fluid Mech.*, *588*, 253, doi:10.1017/S0022112007007525.

Denskat, K. U., and F. M. Neubauer (1982), Statistical properties of low-frequency magnetic field fluctuations in the solar wind from 0.29 to 1.0 AU during solar minimum conditions: HELIOS 1 ad HELIOS 2, *J. Geophys. Res.*, *87*, 2215, doi:10.1029/JA087iA04p02215.

Dimotakis, P. E. (2000), The mixing transition in turbulent flows, *J. Fluid Mech.*, *409*, 69, doi:10.1017/S0022112099007946.

Dimotakis, P. E. (2005), Turbulent mixing, *Annu. Rev. Fluid Mech.*, *37*, 329, doi:10.1146/annurev.fluid.36.050802.122015.

Durban, P. A. (1982), Analysis of the decay of temperature fluctuations in isotropic turbulence, *Phys. Fluids*, *25*, 1326.

Eckart, C. (1948), An analysis of the stirring and mixing process, *Science*, *26*, 597.

Eselevich, M. V., and V. G. Eselevich (2006), Manifestation of the ray structure of the coronal streamer belt in the form of sharp peaks of the solar wind plasma density in the Earth's orbit, *Geomagn. Aeron.*, *46*, 770, doi:10.1134/S0016793206060132.

Eswaran, V., and S. B. Pope (1988), Direct numerical simulations of the turbulent mixing of a passive scalar, *Phys. Fluids*, *31*, 506, doi:10.1063/1.866832.

Eyni, M., and R. Steinitz (1978), Cooling of slow solar wind protons from the Helios 1 experiment, *J. Geophys. Res.*, *83*, 4387, doi:10.1029/JA083iA09p04387.

Feldman, W. C., J. T. Gosling, D. J. McComas, and J. L. Phillips (1993), Evidence for ion jets in the high-speed solar wind, *J. Geophys. Res.*, *98*, 5593, doi:10.1029/92JA02260.

Fox, E. A., and V. E. Gex (1956), Single-phase blending of liquids, *AIChE J.*, *2*, 539, doi:10.1002/aic.690020422.

Freeman, J. W. (1988), Estimates of solar wind heating inside 0.3 AU, *Geophys. Res. Lett.*, *15*, 88, doi:10.1029/GL015i001p00088.

Freeman, J. W., and R. E. Lopez (1985), The cold solar wind, *J. Geophys. Res.*, *90*, 9885, doi:10.1029/JA090iA10p09885.

Garrett, C. (1983), On the initial streakiness of a dispersing tracer in two- and three-dimensional turbulence, *Dyn. Atmos. Oceans*, *7*, 265, doi:10.1016/0377-0265(83)90008-8.

Gibson, C. H. (1991), Kolmogorov similarity hypothesis for scalar fields: Sampling intermittent turbulent mixing in the ocean and galaxy, *Proc. R. Soc. London, Ser. A*, *434*, 149, doi:10.1098/rspa.1991.0086.

Goertz, C. K., and W. Baumjohann (1991), On the thermodynamics of the plasma sheet, *J. Geophys. Res.*, *96*, 20,991, doi:10.1029/91JA02128.

Goldstein, M. L., D. A. Roberts, and W. H. Matthaeus (1995), Magnetohydrodynamic turbulence in the solar wind, *Annu. Rev. Astron. Astrophys.*, *33*, 283, doi:10.1146/annurev.aa.33.090195.001435.

Gosling, J. T. (1999), On the determination of electron polytrope indices within coronal mass ejections in the solar wind, *J. Geophys. Res.*, *104*, 19,851, doi:10.1029/1999JA900254.

Gosling, J. T., J. R. Asbridge, S. J. Bame, and W. C. Feldman (1978), Solar wind stream interfaces, *J. Geophys. Res.*, *83*, 1401, doi:10.1029/JA083iA04p01401.

Hartmann, H., J. J. Derksen, and H. E. A. van den Akker (2006), Mixing times in a turbulent stirred tank by means of LES, *AIChE J.*, *52*, 3696, doi:10.1002/aic.10997.

Hewish, A. (1958), The scattering of radio waves in the solar corona, *Mon. Not. R. Astron. Soc.*, *118*, 534.

Holzer, M., and E. D. Siggia (1994), Turbulent mixing of a passive scalar, *Phys. Fluids*, *6*, 1820, doi:10.1063/1.868243.

Horbury, T. S., and J. M. Schmidt (1999), Development and effects of turbulence in connection with CIRs, *Space Sci. Rev.*, *89*, 61, doi:10.1023/A:1005260331464.

Huq, P., and R. E. Britter (1995), Mixing due to grid-generated turbulence of a two-layer scalar profile, *J. Fluid Mech.*, *285*, 17, doi:10.1017/S0022112095000449.

Joshi, B., and A. Joshi (2004), The north-south asymmetry of soft X-ray flare index during solar cycles 21, 22, and 23, *Sol. Phys.*, *219*, 343, doi:10.1023/B:SOLA.0000022977.95023.a7.

Kepko, L., and H. E. Spence (2003), Observations of discrete, global magnetospheric oscillations directly driven by solar wind density variations, *J. Geophys. Res.*, *108*(A6), 1257, doi:10.1029/2002JA009676.

Kerstein, A. R. (1991), Linear-eddy modeling of turbulent transport. Part V. Geometry of scalar interfaces, *Phys. Fluids A*, *3*, 1110, doi:10.1063/1.858092.

Klein, L., R. Bruno, B. Bavassano, and H. Rosenbauer (1993), Anisotropy and minimum variance of magnetohydrodynamic fluctuations in the inner heliosphere, *J. Geophys. Res.*, *98*, 17,461, doi:10.1029/93JA01522.

Kramers, H., G. M. Baars, and W. H. Knoll (1953), A comparative study of the rate of mixing in stirred tanks, *Chem. Eng. Sci.*, *2*, 35, doi:10.1016/0009-2509(53)80006-0.

Kresta, S. M., and R. S. Brodkey (2003), Turbulence in mixing applications, in *Handbook of Industrial Mixing*, edited by E. L. Paul, V. A. Atiemo-Obeng, and S. M. Kresta, p. 19, Wiley-Interscience, Hoboken, N. J., doi:10.1002/0471451452.ch2.

Kulsrud, R. M. (1983), MHD description of plasmas, in *Handbook of Plasma Physics: Basic Plasma Physics*, edited by M. N. Rosenbluth and R. Z. Sagdeev, p. 123, North-Holland, Amsterdam.

Lee, S. K., L. Djenidi, and R. A. Antonia (2010), Decay of a passive scalar in stretched grid turbulence, paper presented at 17th Australasian Fluid Mechanics Conference, Aust. Fluids Mech. Soc., Aukland, New Zealand.

Li, G., B. Miao, Q. Hu, and G. Qin (2011), Effect of current sheets on the solar wind magnetic field power spectrum from the Ulysses observations: From Kraichnan to Kolmogorov scaling, *Phys. Rev. Lett.*, *106*, 125001, doi:10.1103/PhysRevLett.106.125001.

Liepmann, H. W. (1979), The rise and fall of ideas in turbulence, *Am. Sci.*, *67*, 221.

Livescu, D., and J. R. Ristorcelli (2008), Variable-density mixing in buoyancy-driven turbulence, *J. Fluid Mech.*, *605*, 145, doi:10.1017/S0022112008001481.

Livescu, D., F. A. Jaberi, and C. K. Madnia (2000), Passive-scalar wake behind a line source in grid turbulence, *J. Fluid Mech.*, *416*, 117, doi:10.1017/S0022112000008910.

Luttrell, A. H., and A. K. Richter (1988), The role of Alfvénic fluctuations in MHD turbulence evolution between 0.3 and 1 AU, in *Proceedings of the Sixth International Solar Wind Conference*, *Tech. Note 306*, edited by V. J. Pizzo, T. E. Holzer, and D. G. Sime, p. 335, Natl. Cent. for Atmos. Res., Boulder, Colo.

Mariani, F. B., B. Bavassano, and U. Villante (1983), A statistical study of MHD discontinuities in the inner solar system: Helios 1 and 2, *Sol. Phys.*, *83*, 349, doi:10.1007/BF00148285

Marsch, E., and C.-Y. Tu (1990a), On the radial evolution of MHD turbulence in the inner heliosphere, *J. Geophys. Res.*, *95*, 8211, doi:10.1029/JA095iA06p08211.

Marsch, E., and C.-Y. Tu (1990b), Spectral and spatial evolution of compressible turbulence in the inner solar wind, *J. Geophys. Res.*, *95*, 11,945, doi:10.1029/JA095iA08p11945.

Marsch, E., W. G. Pilipp, K. M. Thieme, and H. Rosenbauer (1989), Cooling of solar wind electrons inside 0.3 AU, *J. Geophys. Res.*, *94*, 6893, doi:10.1029/JA094iA06p06893.

Matsumoto, Y., and M. Hoshino (2006), Turbulent mixing and transport of collisionless plasmas across a stratified velocity shear layer, *J. Geophys. Res.*, *111*, A05213, doi:10.1029/2004JA010988.

Matthaeus, W. H., C. W. Smith, and S. Oughton (1998), Dynamical age of solar wind turbulence in the outer heliosphere, *J. Geophys. Res.*, *103*, 6495, doi:10.1029/97JA03729.

McKelvey, K. N., H.-N. Yieh, S. Zakanycz, and R. S. Brodkey (1975), Turbulent motion, mixing, and kinetics in a chemical reactor configuration, *AIChE J.*, *21*, 1165, doi:10.1002/aic.690210617.

Miller, P. L., and P. E. Dimotakis (1991), Stochastic geometric properties of scalar interfaces in turbulent jets, *Phys. Fluids A*, *3*, 168, doi:10.1063/1.857876.

Miura, A., and P. L. Pritchett (1982), Nonlocal stability analysis of the MHD Kelvin-Helmholtz instability in a compressible plasma, *J. Geophys. Res.*, *87*, 7431, doi:10.1029/JA087iA09p07431.

Neugebauer, M., P. C. Liewer, B. E. Goldstein, X. Zhou, and J. T. Steinberg (2004), Solar wind stream interaction regions without sector boundaries, *J. Geophys. Res.*, *109*, A10102, doi:10.1029/2004JA010456.

Newman, G. R., Z. Warhaft, and J. M. Lumley (1977), The decay of temperature fluctuations in isotropic turbulence, paper presented at Sixth Australian Hydraulics and Fluid Mechanics Conference, U.S. Environ. Prot. Agency, Adelaide, Australia.

Norwood, K. W., and A. B. Metzner (1960), Flow patterns and mixing rates in agitated vessels, *AIChE J.*, *6*, 432, doi:10.1002/aic.690060317.

Ofman, L. (2004), The origin of the slow solar wind in coronal streamers, *Adv. Space Res.*, *33*, 681, doi:10.1016/S0273-1177(03)00235-7.

Ogilvie, K. W., M. A. Coplan, D. A. Roberts, and F. Ipavich (2007), Solar wind structure suggested by bimodal correlations of solar wind speed and density between the spacecraft SOHO and Wind, *J. Geophys. Res.*, *112*, A08104, doi:10.1029/2007JA012248.

Osherovich, V. A., J. Fainberg, R. G. Stone, R. J. MacDowall, and D. Berdichevsky (1997), Self-similar evolution of interplanetary magnetic clouds and Ulysses measurements of the polytropic index inside the cloud, *Eur. Space Agency Spec. Publ.*, *ESA SP-415*, 171.

Ottino, J. M. (1990), Mixing, chaotic advection, and turbulence, *Annu. Rev. Fluid Mech.*, *22*, 207, doi:10.1146/annurev.fl.22.010190.001231.

Ottino, J. M., C. W. Leong, H. Rising, and P. D. Swanson (1988), Morphological structures produced by mixing in chaotic flows, *Nature*, *333*, 419, doi:10.1038/333419a0.

Owens, M. J., R. T. Wicks, and T. S. Horbury (2011), Magnetic discontinuities in the near-Earth solar wind: Evidence of in-transit turbulence or remnants of coronal structure?, *Sol. Phys.*, *269*, 411, doi:10.1007/s11207-010-9695-0.

Pagel, A. C., N. U. Crooker, T. H. Zurbuchen, and J. T. Gosling (2004), Correlation of solar wind entropy and oxygen ion charge state ratio, *J. Geophys. Res.*, *109*, A01113, doi:10.1029/2003JA010010.

Paul, E. L., V. A. Atiemo-Obeng, and S. M. Kresta (Eds.) (2003), *Handbook of Industrial Mixing*, Wiley-Interscience, Hoboken, N. J., doi:10.1002/0471451452.

Pizzo, V. (1978), A three-dimensional model of corotating streams in the solar wind: 1. Theoretical foundations, *J. Geophys. Res.*, *83*, 5563, doi:10.1029/JA083iA12p05563.

Prasad, R. R., and K. R. Sreenivasan (1989), Scalar interfaces in digital images of turbulent flows, *Exp. Fluids*, *7*, 259, doi:10.1007/BF00198005.

Prasad, R. R., and K. R. Sreenivasan (1990), The measurement of interpretation of fractal dimensions of the scalar interface in turbulent flows, *Phys. Fluids A*, *2*, 792, doi:10.1063/1.857733.

Prochazka, J., and J. Landau (1961), Studies on mixing. XII. Homogenation of miscible liquids in the turbulent region, *Collect. Czech. Chem. Commun.*, *26*, 2961.

Rehme, K. (1992), The structure of turbulence in rod bundles and the implications on natural mixing between the subchannels, *Int. J. Heat Mass Transfer*, *35*, 567, doi:10.1016/0017-9310(92)90291-Y.

Reisenfeld, D. B., D. J. McComas, and J. T. Steinberg (1999), Evidence of a solar origin for pressure balance structures in the high-latitude solar wind, *Geophys. Res. Lett.*, *26*, 1805, doi:10.1029/1999GL900368.

Richardson, J. D., and K. I. Paularena (1998), The orientation of plasma structure in the solar wind, *Geophys. Res. Lett.*, *25*, 2097, doi:10.1029/98GL01520.

Richardson, J. D., and K. I. Paularena (2001), Plasma and magnetic field correlations in the solar wind, *J. Geophys. Res.*, *106*, 239, doi:10.1029/2000JA000071.

Ridley, A. J. (2000), Estimations of the uncertainty in timing the relationship between magnetospheric and solar wind processes, *J. Atmos. Sol. Terr. Phys.*, *62*, 757, doi:10.1016/S1364-6826(00)00057-2.

Ristorcelli, J. R. (2006), Passive scalar mixing: Analytic study of time scale ratio, variance, and mix rate, *Phys. Fluids*, *18*, 075101, doi:10.1063/1.2214704.

Roberts, D. A. (2010), The evolution of the spectrum of solar wind magnetic and velocity fluctuations from 0.3 to 5 AU, *J. Geophys. Res.*, *115*, A12101, doi:10.1029/2009JA015120.

Roberts, D. A., M. L. Goldstein, W. H. Matthaeus, and S. Ghosh (1992), Velocity shear generation of solar wind turbulence, *J. Geophys. Res.*, *97*, 17,115, doi:10.1029/92JA01144.

Rosenbauer, H., R. Schwenn, E. Marsch, B. Meyer, H. Miggenrieder, M. D. Montgomery, K. H. Muhlhauser, W. Pilipp, W. Voges, and S. M. Zink (1977), A survey on initial results of the Helios plasma experiment, *J. Geophys. Res.*, *42*, 561.

Sari, J. W., and N. F. Ness (1969), Power spectra of the interplanetary magnetic field, *Sol. Phys.*, *8*, 155, doi:10.1007/BF00150667.

Schindler, K., and J. Birn (1978), Magnetospheric physics, *Phys. Rep.*, *47*, 109, doi:10.1016/0370-1573(78)90016-9.

Schwenn, R. (1990), Large scale structure of the interplanetary medium, in *Physics of the Inner Heliosphere I*, edited by R. Schwenn and E. Marsch, p. 99, Springer, Berlin.

Schwenn, R., K.-H. Muhlhauser, E. Marsch, and H. Rosenbauer (1981), Two states of the solar wind at the time of solar activity minimum: II. Radial gradients of plasma parameters in fast and slow streams, in *Solar Wind Four*, *MPAE-W-100-81-31*, p. 126, Max Planck Inst. fur Aeron., Lindau, Germany.

Seale, W. J. (1979), Turbulent diffusion of heat between connected flow passages, *Nucl. Eng. Design*, *54*, 197, doi:10.1016/0029-5493(79)90167-5.

Shraiman, B. I., and E. D. Siggia (2000), Scalar turbulence, *Nature*, *405*, 639, doi:10.1038/35015000.

Siscoe, G. L., L. Davis, P. J. Coleman, E. J. Smith, and D. E. Jones (1968), Power spectra and discontinuities of the interplanetary magnetic field: Mariner 4, *J. Geophys. Res.*, *73*, 61, doi:10.1029/JA073i001p00061.

Sreenivasan, K. R., and R. A. Antonia (1997), The phenomenology of small-scale turbulence, *Annu. Rev. Fluid Mech.*, *29*, 435, doi:10.1146/annurev.fluid.29.1.435.

Sreenivasan, K. R., S. Tavoularis, R. Henry, and S. Corrsin (1980), Temperature fluctuations in grid-generated turbulence, *J. Fluid Mech.*, *100*, 597, doi:10.1017/S0022112080001309.

Sreenivasan, K. R., A. Prabhu, and R. Narasimha (1983), Zero-crossings in turbulent signals, *J. Fluid Mech.*, *137*, 251, doi:10.1017/S0022112083003396.

Stapountzis, H., B. L. Sawford, J. C. R. Hunt, and R. E. Britter (1986), Structure of the temperature field downwind of a line source in grid turbulence, *J. Fluid Mech.*, *165*, 401, doi:10.1017/S0022112086003154.

Thieme, K. M., E. Marsch, and R. Schwenn (1988), Relationship between structures in the solar wind and their source regions in the corona, in *Proceedings of the Sixth International Solar Wind Conference*, *Tech. Note 306*, edited by V. J. Pizzo, T. Holzer, and D. G. Sime, p. 317, Natl. Cent. for Atmos. Res., Boulder, Colo.

Thieme, K. M., R. Schwenn, and E. Marsch (1989), Are structures in high-speed streams signatures of coronal fine structures?, *Adv. Space Res.*, *9*(4), 127, doi:10.1016/0273-1177(89)90105-1.

Thieme, K. M., E. Marsch, and R. Schwenn (1990), Spatial structures in high-speed streams as signatures of fine structures in coronal holes, *Ann. Geophys.*, *8*, 713.

Tu, C.-Y., and E. Marsch (1991), A case study of very low cross-helicity fluctuations in the solar wind, *Ann. Geophys.*, *9*, 319.

Tu, C.-Y., and E. Marsch (1994), On the nature of compressive fluctuations in the solar wind, *J. Geophys. Res.*, *99*, 21,481, doi:10.1029/94JA00843.

Tu, C.-Y., and E. Marsch (1995), MHD structures, waves and turbulence in the solar wind, *Space Sci. Rev.*, *73*, 1, doi:10.1007/BF00748891.

Tu, C.-Y., E. Marsch, and H. Rosenbauer (1990), The dependence of MHD turbulence spectra on the inner solar wind stream structure near solar minimum, *Geophys. Res. Lett.*, *17*, 283, doi:10.1029/GL017i003p00283.

Viall, N. M., H. E. Spence, and J. Kasper (2009a), Are periodic solar wind number density structures formed in the solar corona?, *Geophys. Res. Lett.*, *36*, L23102, doi:10.1029/2009GL041191.

Viall, N. M., L. Kepko, and H. E. Spence (2009b), Relative occurrence rates and connection of discrete frequency oscillations in the solar wind density and dayside magnetosphere, *J. Geophys. Res.*, *114*, A01201, doi:10.1029/2008JA013334.

Viall, N. M., H. E. Spence, A. Vourlidas, and R. Howard (2010), Examining periodic solar-wind density structures observed in the SECCHI heliospheric imagers, *Sol. Phys.*, *267*, 175, doi:10.1007/s11207-010-9633-1.

Villante, U., P. Francia, M. Vellante, P. Di Giuseppe, A. Nubile, and M. Pirsanti (2007), Long-period oscillations at discrete frequencies: A comparative analysis of ground, magnetospheric, and interplanetary observations, *J. Geophys. Res.*, *112*, A04210, doi:10.1029/2006JA011896.

Villermaux, E., and C. Innocenti (1999), On the geometry of turbulent mixing, *J. Fluid Mech.*, *393*, 123, doi:10.1017/S0022112099005674.

Villermaux, E., C. Innocenti, and J. Duplat (1998), Historgramme des fluctuations scalaires dans le mélange turbulent transitoire, *Comp. Rend. Acad. Sci. Paris*, *326*, 21.

Voth, G. A., T. C. Saint, G. Dobler, and J. P. Gollub (2003), Mixing rates and symmetry breaking in two-dimensional chaotic flow, *Phys. Fluids*, *15*, 2560, doi:10.1063/1.1596915.

Wang, Y.-M., N. R. Sheeley, D. G. Socker, R. A. Howard, and N. B. Rich (2000), The dynamical nature of coronal streamers, *J. Geophys. Res.*, *105*, 25,133, doi:10.1029/2000JA000149.

Warhaft, Z. (2000), Passive scalars in turbulent flows, *Annu. Rev. Fluid Mech.*, *32*, 203, doi:10.1146/annurev.fluid.32.1.203.

Weimer, D. R., and J. H. King (2008), Improved calculations of interplanetary magnetic field phase front angles and propagation time delays, *J. Geophys. Res.*, *113*, A01105, doi:10.1029/2007JA012452.

Whang, Y. C., K. W. Behannon, L. F. Burlaga, and S. Zhang (1989), Thermodynamic properties of the heliospheric plasma, *J. Geophys. Res.*, *94*, 2345, doi:10.1029/JA094iA03p02345.

Wicks, R. T., M. J. Owens, and T. S. Horbury (2010), The variations of solar wind correlation lengths over three solar cycles, *Sol. Phys.*, *262*, 191, doi:10.1007/s11207-010-9509-4.

Woo, R., and S. R. Habbal (1997), Extension of coronal structure into interplanetary space, *Geophys. Res. Lett.*, *24*, 1159, doi:10.1029/97GL01156.

Woo, R., and S. R. Habbal (1998), Multiscale filamentary structures in the solar corona and their implications for the origin and evolution of the solar wind, *Phys. Space Plasmas*, *15*, 351.

Yamauchi, Y., S. T. Suess, and T. Sakurai (2002), Relation between pressure balance structures and polar plums from Ulysses high-latitude observations, *Geophys. Res. Lett.*, *29*(10), 1383, doi:10.1029/2001GL013820.

Yamauchi, Y., S. T. Suess, and T. Sakurai (2003), Relation between polar plums and fine structure in the solar wind from Ulysses high-latitude observations, *AIP Conf. Proc.*, *679*, 255, doi:10.1063/1.1618589.

Yee, E., R. Chan, P. R. Kosteniuk, G. M. Chandler, C. A. Biltoft, and J. F. Bowers (1995a), Measurement of level-crossing statistics of concentration fluctuation statistics in plumes dispersing in the atmospheric surface layer, *Boundary Layer Meteorol.*, *73*, 53, doi:10.1007/BF00708930.

Yee, E., R. Chan, P. R. Kosteniuk, G. M. Chandler, C. A. Biltoft, and J. F. Bowers (1995b), The vertical structure of concentration fluctuation statistics in plumes dispersing in the atmospheric surface layer, *Boundary Layer Meteorol.*, *76*, 41, doi:10.1007/BF00710890.

Yeung, P. K. (2002), Lagrangian investigations of turbulence, *Annu. Rev. Fluid Mech.*, *34*, 115, doi:10.1146/annurev.fluid.34.082101.170725.